

# Novel Indenoisoquinolines NSC 725776 and NSC 724998 Produce Persistent Topoisomerase I Cleavage Complexes and Overcome Multidrug Resistance

Smitha Antony,<sup>1</sup> Keli K. Agama,<sup>1</sup> Ze-Hong Miao,<sup>1</sup> Kazutaka Takagi,<sup>1</sup> Mollie H. Wright,<sup>2</sup> Ana I. Robles,<sup>2</sup> Lyuba Varticovski,<sup>2</sup> Muthukaman Nagarajan,<sup>3</sup> Andrew Morrell,<sup>3</sup> Mark Cushman,<sup>3</sup> and Yves Pommier<sup>1</sup>

<sup>1</sup>Laboratory of Molecular Pharmacology and <sup>2</sup>Laboratory of Human Carcinogenesis, National Cancer Institute, NIH, Bethesda, Maryland and <sup>3</sup>Department of Medicinal Chemistry and Molecular Pharmacology, and the Purdue Cancer Center, Purdue University, West Lafayette, Indiana

## Abstract

**Camptothecin (CPT) derivatives are effective anticancer drugs, especially against solid tumors. As CPTs are chemically unstable and have clinical limitations, we have synthesized indenoisoquinolines as novel topoisomerase I (Top1) inhibitors. We presently report two indenoisoquinoline derivatives, NSC 725776 and NSC 724998, which have been selected for therapeutic development. Both are potent Top1 inhibitors and induce Top1 cleavage at unique genomic positions compared with CPT. Consistent with Top1 poisoning, protein-linked DNA breaks were detected in cells treated with NSC 725776 and NSC 724998 at nanomolar concentrations. Those drug-induced protein-linked DNA breaks persisted longer after drug removal than those produced by CPT. Studies in human cells in culture show that NSC 725776 and NSC 724998 exert antiproliferative activity at submicromolar concentrations. Furthermore, NSC 725776 and NSC 724998 show cross-resistance in cells deficient or silenced for Top1, which is consistent with their selective Top1 targeting. Similar to other known Top1 inhibitors, NSC 725776–treated and NSC 724998–treated cells show an arrest of cell cycle progression in both S and G<sub>2</sub>-M and a dependence on functional p53 for their cytotoxicity. Dose-dependent  $\gamma$ -H2AX foci formation was readily observed in cells treated with NSC 725776 and NSC 724998. These  $\gamma$ -H2AX foci were detectable at pharmacologically relevant doses for up to 24 h and thus could be used as biomarkers for clinical trials (phase 0). [Cancer Res 2007; 67(21):10397–405]**

## Introduction

Camptothecin (CPT) derivatives, which selectively target DNA topoisomerase I (Top1; refs. 1–3), are among the most effective anticancer drugs recently approved by the U.S. Food and Drug Administration (FDA), especially against solid tumors (4). However, CPTs have limitations. They are chemically unstable, as the  $\alpha$ -hydroxylactone in the E-ring is rapidly converted to a carboxylate whose tight binding to human serum albumin limits the available active drug (4–6). CPT diffuses rapidly from the Top1 cleavage

complexes (5, 7), resulting in the need for prolonged infusions to maintain persistent cleavage complexes. In addition, CPTs are actively exported from the cell by drug efflux membrane “pumps” (8). The fact that CPTs are the only class of Top1 poisons used in the clinic to date prompted us to search for novel Top1 inhibitors. Following a COMPARE analysis of the National Cancer Institute (NCI) drug screen database using CPT as a seed, we identified an indenoisoquinoline (NSC 314622) as a Top1 inhibitor (Fig. 1; ref. 9). NSC 314622 served as a lead compound for the development of indenoisoquinolines to overcome some of the limitations of CPTs and to develop novel classes of Top1 inhibitors with different anticancer activity profiles. We have now synthesized and tested >300 indenoisoquinoline derivatives and found that some of them are both very potent Top1 poisons and exhibit antitumor activity in mouse models (10–13). We have also obtained crystal structures of two different indenoisoquinolines within Top1 cleavage complexes (14–16).

One of our goals is to maximize the antiproliferative activities of indenoisoquinolines in human cancer cell cultures as well as their activities as Top1 inhibitors both *in vitro* and *in vivo*. Additionally, to overcome some of the clinical limitations imposed by CPT derivatives, we aim to generate derivatives that (a) are chemically stable, (b) have a distinct DNA cleavage pattern, (c) would produce Top1-DNA cleavage complexes that persist longer in cells than those trapped by CPT, and (d) would be limited substrates for the drug efflux membrane pumps multidrug resistance (MDR)-1 (P-glycoprotein) and ABCG2 compared with the clinical derivatives of CPT (8, 17). Here, we presently report two novel indenoisoquinoline derivatives, NSC 725776 and NSC 724998 (Fig. 1), which satisfy these criteria. These two drugs along with NSC 706744 (Fig. 1; refs. 13, 18) have been selected by the NCI Developmental Therapeutics Program for clinical development.

As CPT binds reversibly to Top1 cleavage complexes (5, 7, 19), CPT does not directly damage DNA. However, on collision with a replication fork or the transcription machinery, those reversible CPT-DNA-Top1 cleavage complexes are converted into irreversible Top1 covalent complexes and, subsequently, DNA damage (double-strand breaks), which, if not repaired, leads to cell death (4). Thus, replication fork collision is the primary cytotoxic mechanism of CPT in dividing cells. One of the well-characterized molecular responses to replication double-strand breaks is the phosphorylation of the H2AX histone variant. The phosphorylated form of H2AX, termed  $\gamma$ -H2AX, is observed within minutes after the formation of CPT-induced replication double-strand breaks (20, 21).  $\gamma$ -H2AX can be detected by immunofluorescence or immunostaining, as it accumulates and forms a nuclear focus

**Note:** Supplementary data for this article are available at Cancer Research Online (<http://cancerres.aacrjournals.org/>).

**Requests for reprints:** Yves Pommier, Laboratory of Molecular Pharmacology, National Cancer Institute, 37 Convent Drive, Building 37, Room 5068, NIH, Bethesda, MD 20892-4255. Phone: 301-496-5944; Fax: 301-402-0752; E-mail: [pommier@nih.gov](mailto:pommier@nih.gov).

©2007 American Association for Cancer Research.

doi:10.1158/0008-5472.CAN-07-0938

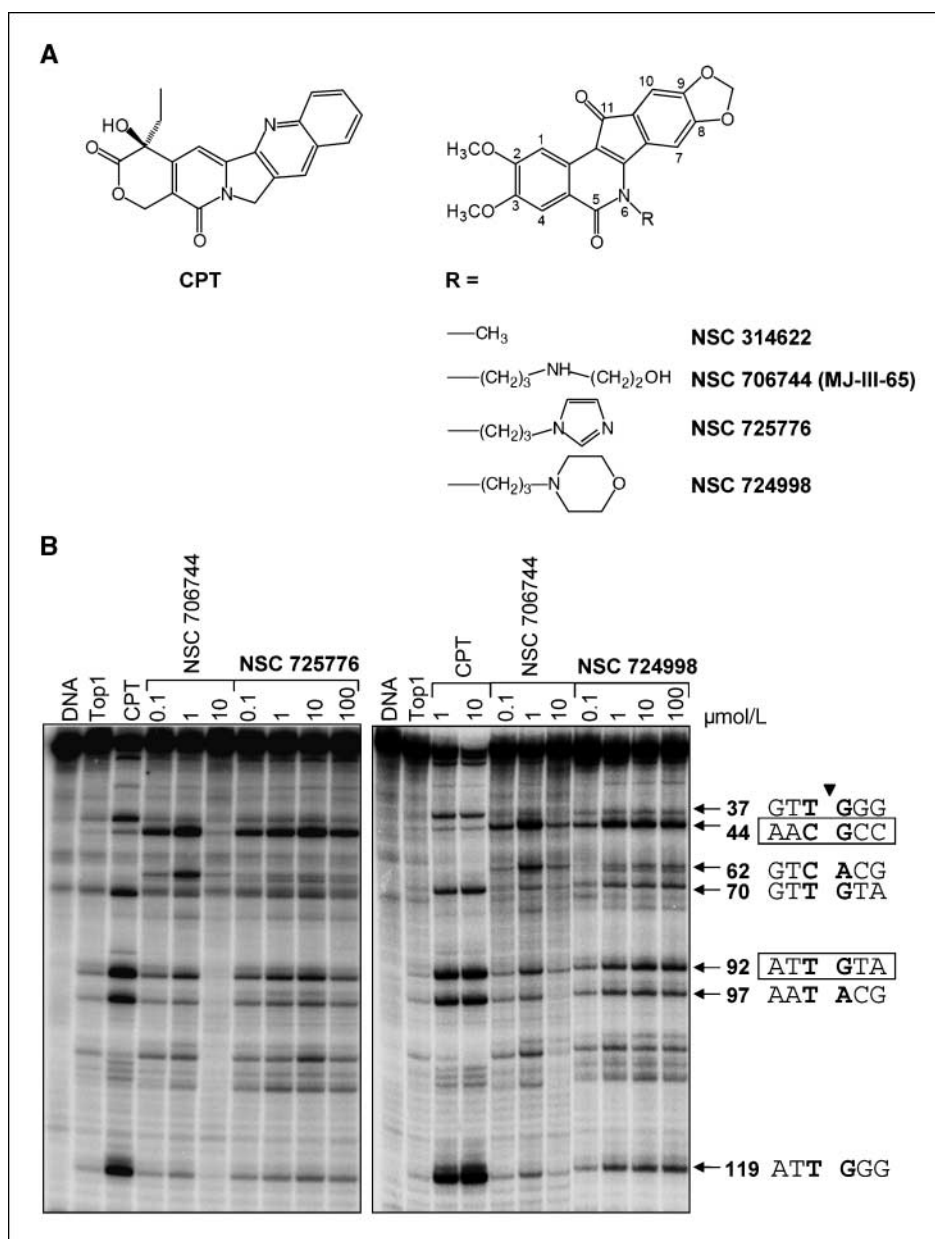


**Figure 1.** The indenoisoquinolines NSC 725776 and NSC 724998 trap Top1-DNA cleavage complexes. **A**, chemical structures of the indenoisoquinolines NSC 725776, NSC 724998, MJ-III-65 (NSC 706744; refs. 13, 18) and NSC 314622 (the parent indenoisoquinoline; refs. 9), and CPT. **B**, the DNA corresponds to the 3'-end labeled *PvuII/HindIII* fragment of pSK. DNA was reacted with Top1 in the absence of drug (Top1) or in the presence of the indicated concentrations ( $\mu\text{mol/L}$ ) of CPT, NSC 706744, or NSC 725776 (*left*) and NSC 724998 (*right*). Reactions were at 25°C for 20 min and stopped by adding 0.5% SDS. DNA fragments were separated in 16% denaturing polyacrylamide gels. *Numbers to the side of the gel*, migration positions of DNA fragments cleaved at these positions by Top1 in the pSK DNA. The base sequences encompassing the cleavage sites are represented, with the bases flanking the cleavage site highlighted in bold. Boxed sequences represent the most preferred sites of Top1-mediated cleavage trapped by both NSC 725776 and NSC 724998.

around each double-strand break.  $\gamma$ -H2AX can be also detected by fluorescence-activated cell sorting (20, 21).  $\gamma$ -H2AX is an extremely sensitive marker for double-strand breaks that are produced not only by DNA-damaging agents but also by genomic instability and apoptosis (22). Consequently, we wanted to evaluate whether  $\gamma$ -H2AX can be used as a biomarker to monitor the activity of the indenoisoquinolines NSC 725776 and NSC 724998.

The present study elucidates the cellular and molecular effects of NSC 725776 and NSC 724998 as potent Top1 inhibitors. As the indenoisoquinolines advance among the first candidates for phase 0 clinical trials (23),  $\gamma$ -H2AX can be used as a clinical marker for monitoring the efficacy of NSC 725776 and NSC 724998.

## Materials and Methods

**Drugs, enzymes, and chemicals.** CPT, topotecan, and SN-38 were obtained from the Drug Synthesis and Chemistry Branch, NCI (Bethesda, MD). The syntheses of NSC 314622 (24), MJ-III-65 (NSC 706744; ref. 10), NSC

725776, and NSC 724998 have been previously described (25). Recombinant human Top1 (Top1) was purchased from TopoGEN, Inc. Recombinant yeast topoisomerase II (Top2) was a kind gift from Dr. John Nitiss (St. Jude's Children's Research Hospital, Memphis, TN). DNA polymerase I (Klenow fragment), T4 polynucleotide kinase, deoxynucleotide triphosphate [where N is A (adenosine), C (cytosine), G (guanosine), or T (thymine)], and polyacrylamide/bis were purchased from Invitrogen. DNA quick spin columns were purchased from Roche Diagnostics Corp. [ $\alpha$ - $^{32}\text{P}$ ]dGTP and [ $\gamma$ - $^{32}\text{P}$ ]dATP were purchased from DuPont-New England Nuclear.

**Top1 and Top2 cleavage assays.** The 161-bp fragment from pBluescript SK(-) phagemid DNA (pSK; Stratagene) was 3'-end labeled with [ $\alpha$ - $^{32}\text{P}$ ]dGTP or 5'-end labeled with [ $\gamma$ - $^{32}\text{P}$ ]dATP for Top1 and Top2 cleavage assays, respectively. Cleavage assays were carried out as described previously (18, 26).

**Alkaline elution assay for the detection of DNA-protein cross-links.** Alkaline elution was done to assess DNA damage by detecting DNA-protein cross-links (DPC) as previously described (27). Radiolabeled human leukemic CEM cells were treated for 1 h with 1  $\mu\text{mol/L}$  of NSC 725776 or NSC 724998 or CPT or topotecan or SN-38. For reversal, after 1 h of drug

treatment, the cells were cultured in drug-free medium for the appropriate time. DPCs were analyzed under nondeproteinizing, DNA-denaturing conditions using protein-adsorbing filters and the DPC frequencies were calculated as described previously (13, 26).

**Detection of covalent Top1-DNA complexes in CEM cells.** Top1-DNA adducts were isolated using the immunocomplex of enzyme (ICE) bioassay (28–30). Top1-DNA complexes were detected using the C21 Top1 monoclonal antibody (a kind gift from Dr. Yung-Chi Cheng, Yale University, New Haven, CT) by standard Western procedures.

**Confocal microscopy.** Laser scanning confocal microscopy was done as described (21). HT29 cells were grown in culture medium on chamber slides. After drug treatment, HT29 cells were fixed with paraformaldehyde and washed in PBS and then permeabilized in 100% methanol. Slides were blocked for 1 h with PBS containing 1% bovine serum albumin (BSA) and 5% goat serum (Jackson Immunolaboratories), incubated with anti- $\gamma$ -H2AX antibody (Upstate), washed, incubated for 1 h with Alexa Fluor 488-conjugated goat anti-mouse IgG secondary antibody (Molecular Probes) at a 200-fold dilution, and washed in PBS. The slides were stained with propidium iodide, sealed with mounting medium (Vectashield, Vector Laboratories, Inc.), and viewed using a PCM2000 laser scanning confocal microscope (Nikon Co.) with a  $\times 40$  objective.

**Flow cytometry analysis of DNA content.** Cell cycle analyses of HT29 cells treated with 0.01, 0.05, 0.1, or 0.5  $\mu\text{mol/L}$  of NSC 725776 or NSC 724998 were done with a FACScan flow cytometer (Becton Dickinson; refs. 13, 26). Cell cycle distributions were calculated using ModFit LT software (Verity Software House, Inc.).

**Two-dimensional flow cytometry analysis: DNA content and  $\gamma$ -H2AX staining.** HT29 cells were treated for 1 h with 1  $\mu\text{mol/L}$  of CPT or NSC 725776 or NSC 724998. After treatment, the cells were harvested, washed twice with ice-cold PBS, fixed in 4% paraformaldehyde for 10 min at room temperature, and postfixed with 70% ethanol overnight at 4°C. The cells were washed in PBS and then suspended in 400  $\mu\text{L}$  of mouse- $\gamma$ -H2AX antibody (1:500 dilution in PBS, 1% BSA) and incubated for 1 h at room temperature. The cells were spun down and washed twice with PBS and then resuspended in 400  $\mu\text{L}$  of anti-mouse Alexa Fluor 488 antibody (1:500 dilution in PBS, 1% BSA) for 30 min at room temperature but protected from light. The pellet was then washed twice with PBS and counterstained with propidium iodide (50  $\mu\text{g/mL}$ ) containing RNaseA (0.5 mg/mL) for 30 min, and analyses of FL2-A (propidium iodide) versus FL1-H ( $\gamma$ -H2AX) were done with a FACScan flow cytometer.

**Cell lines and cytotoxicity assays.** P388 and P388 Top1-deficient murine leukemia cells (31) were a kind gift from Michael R. Mattern and Randal K. Johnson (GlaxoSmithKline) and were maintained in RPMI 1640 (Invitrogen) containing 10% fetal bovine serum (FBS; Atlanta Biologicals). Human colon HCT-116 and breast cancer MCF-7 cells were purchased from the American Type Culture Collection (ATCC). The stably transfected HCT-116 Top1-small interfering RNA (siRNA; HCT-116-siTop1) and MCF-7 Top1-siRNA (MCF-7-siTop1) cells were derived as described (30, 32). HCT-116 and MCF-7 cells were maintained in DMEM supplemented with 10% FBS. TK6 and NH32 are EBV-immortalized human lymphoblastoid cell lines (gift of Dr. Howard Liber, Colorado State University, Fort Collins, CO) and were maintained in RPMI 1640 supplemented with 10% FBS, glutamine (0.3  $\mu\text{g/mL}$ ), and 1% penicillin/streptomycin. TK6 has wild-type p53 and NH32 is an isogenic cell line generated by p53-targeted deletion and expresses no p53 protein. Human embryonic kidney cells HEK-293 stable transfectants expressing wild-type ABCG2 (HEK-293-R482-5 cells) and wild-type MDR-1/P-glycoprotein (HEK-293-MDR-19 cells; ref. 33) were a kind gift from Dr. Susan E. Bates (NIH, Bethesda, MD) and were maintained in Eagle's MEM (ATCC) supplemented with 10% FBS and G418 (2 mg/mL). All cells were maintained in a 5% CO<sub>2</sub> incubator at 37°C.

Cytotoxicity of NSC 725776 and NSC 724998 in wild-type P388 and P388 Top1-deficient cells was assessed by 3-(4,5-dimethylthiazol-2-yl)-2,5-diphenyltetrazolium bromide (MTT; Sigma-Aldrich Co.) colorimetric assay as described (13). Their cytotoxicity in HCT-116, HCT-116-siTop1, MCF-7, MCF-7-siTop1, HEK-293-R482-5, and HEK-293-MDR-19 cells was assessed by the sulforhodamine B (SRB; Sigma-Aldrich) assay (33). Drug treatment was continuous for 3 days for both the MTT and SRB assays. Determinations for

all experiments were made in duplicates, and the results were expressed as mean  $\pm$  SD. Percentage of growth was calculated relative to control (vehicle-treated cells) after 3 days of culture with control taken as 100. Growth inhibition assay of nonadherent TK6 and NH32 cell lines was assessed by the 3-(4,5-dimethylthiazol-2-yl)-5-(3-carboxymethoxyphenyl)-2-(4-sulfophenyl)-2H-tetrazolium salt (Promega) assay, where cells were treated with drugs for 24 h (26).

## Results

**NSC 725776 and NSC 724998 induce Top1-DNA covalent complexes.** Figure 1A shows the induction of DNA cleavage complexes by NSC 725776 and NSC 724998 in the presence of Top1 as tested in the *PvuII/HindIII* fragment of pSK. Both NSC 725776 and NSC 724998 induced DNA cleavage complexes. Several cleavage sites were similar to those trapped by CPT but with differences in their relative intensities (see sites 70, 92, 97, and 119 in Fig. 1B). Unlike CPT, NSC 725776 and NSC 724998 showed a strong preference for site 44. Site 44 is also preferred by the indenoisoquinoline NSC 706744 (MJ-III-65; ref. 18). However, NSC 725776 and NSC 724998, unlike NSC 706744, showed no cleavage at site 62. To evaluate the effect of NSC 725776 and NSC 724998 on Top2-mediated cleavage, similar cleavage assays were carried out with 5'-labeled pSK DNA. Both NSC 725776 and NSC 724998 showed weak activity against Top2 only at high concentrations and at limited sites (see Supplementary Fig. S1).

These results suggest that the indenoisoquinolines NSC 725776 and NSC 724998 at pharmacologically relevant doses are primarily Top1 poisons with DNA cleavage patterns exhibiting similarities and differences from those of CPT and NSC 706744.

**Induction of Top1-DNA complexes by NSC 725776 and NSC 724998 in cells.** To determine whether NSC 725776 and NSC 724998 induced Top1 cleavage complexes in drug-treated cells, we used the ICE assay (28, 29, 34). Exponentially growing CEM cells were treated for 1 h with 1  $\mu\text{mol/L}$  of NSC 725776 or NSC 724998 or CPT and processed in the ICE bioassay. Fractionation of the cesium chloride gradient (fractions 6–9) and immunoblotting for DNA-containing fractions revealed the presence of Top1 signals in these DNA fractions for the NSC 725776-treated, NSC 724998-treated, and CPT-treated cells but not in the untreated cells (Fig. 2A). These Top1 cleavage complexes were also confirmed by alkaline elutions that detect DPCs (4, 5, 35). NSC 725776 and NSC 724998 produced DPCs in a concentration-dependent manner (data not shown). These experiments indicate that NSC 725776 and NSC 724998 produce Top1-DNA cleavage complexes in cells and show that Top1 is a cellular target of NSC 725776 and NSC 724998.

**Persistence of DPCs induced by NSC 725776 and NSC 724998 in cells after drug removal.** We then studied the persistence of NSC 725776-induced and NSC 724998-induced Top1 cleavage complexes by DPC reversal kinetics. Figure 2B shows that most NSC 725776-induced DPCs were not reversible within 1 h after drug removal ( $R_{60}$ ). NSC 724998-induced DPCs also persisted at 1 h despite significant reversal. By contrast, CPT- and topotecan-induced DNA cross-links reversed completely (Fig. 2B), which is consistent with >90% reversal within 15 min of CPT removal (5, 36). Similarly, SN-38-induced DNA cross-links also reversed following drug removal, albeit more slowly (36). Thus, the Top1 cleavage complexes induced by NSC 725776 and NSC 724998 persist longer than those induced by CPT and its clinical derivatives following drug removal.

**Cytotoxicity of NSC 725776 and NSC 724998 is Top1 dependent.** To evaluate the role Top1 plays in the cytotoxicity of

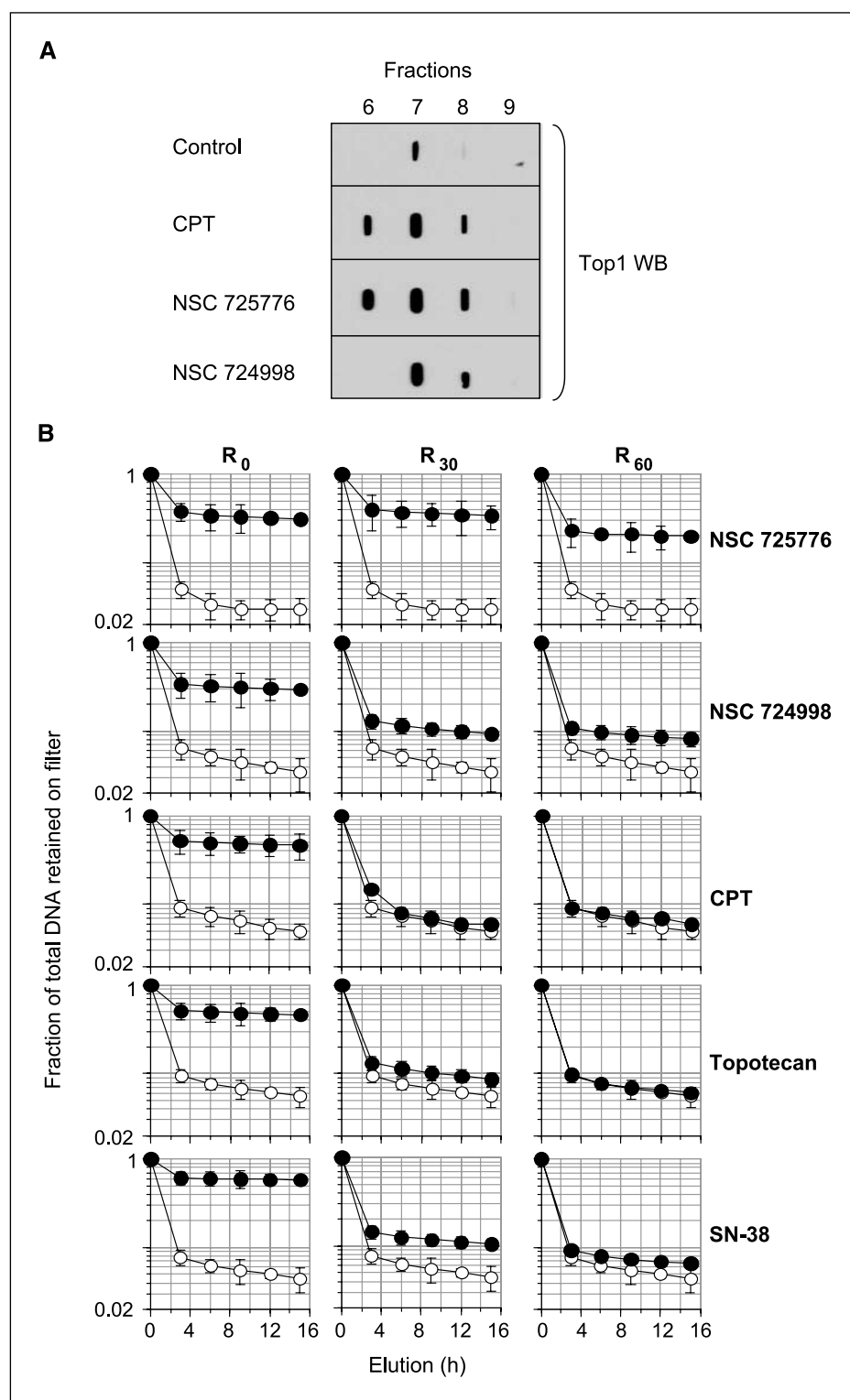


**Figure 2.** Induction of Top1 cleavage complexes and persistent DPCs by NSC 725776 and NSC 724998 in human leukemic CEM cells. **A**, cells were treated with 1  $\mu\text{mol/L}$  of CPT, NSC 725776, or NSC 724998 for 1 h at 37°C. Equal numbers of cells were lysed in 1% sarkosyl and submitted to the ICE assay (see Materials and Methods). DNA-containing fractions were collected from the bottom of the gradients. Fractions (6–9) were blotted, and Top1-DNA covalent complexes were detected using Top1 C21 monoclonal antibody. **B**, cells were prelabeled with [ $^{14}\text{C}$ ]thymidine and treated with either 1  $\mu\text{mol/L}$  NSC 725776 or NSC 724998 or CPT or topotecan or SN-38 for 1 h at 37°C. DPCs were assayed immediately before drug removal ( $R_0$ ) and after drug treatment followed by culturing in drug-free medium for 30 min ( $R_{30}$ ) or 60 min ( $R_{60}$ ), respectively. ●, DPCs induced by NSC 725776, NSC 724998, CPT, topotecan, and SN-38. Points, average of two independent experiments; bars, SD. ○, elution of untreated cells.

NSC 725776 and NSC 724998, Top1-deficient and Top1-siRNA cells were used. The stably transfected Top1-siRNA knockdown cells show a reduction of Top1 (approximately 4- to 5-fold decrease in Top1 levels). Those cells will be described elsewhere (32). As observed in Fig. 3A and B, both NSC 725776 and NSC 724998 were cytotoxic to the wild-type P388 ( $\text{IC}_{50}$ , 25 and 300 nmol/L), MCF-7 ( $\text{IC}_{50}$ , 93 and 560 nmol/L), and HCT-116 ( $\text{IC}_{50}$ , 125 nmol/L and 1.2

$\mu\text{mol/L}$ ) cells. NSC 725776 was more potent than NSC 724998 in all the three cell pairs examined. Despite the difference in the cytotoxic potency of NSC 725776 and NSC 724998, the Top1-deficient P388 cells (13) and the Top1-silenced MCF-7-siTop1 and HCT-116-siTop1 cells showed resistance to both of them. The fold resistance for NSC 725776 and NSC 724998 are >4- and >33-fold in Top1-deficient P388, 11- and 4-fold in MCF-7-siTop1, and 7- and

3-fold in HCT-116-siTop1 cells, respectively (Fig. 3B). These results show that although additional targets may exist, NSC 725776-mediated and NSC 724998-mediated cell killing is primarily dependent on Top1.

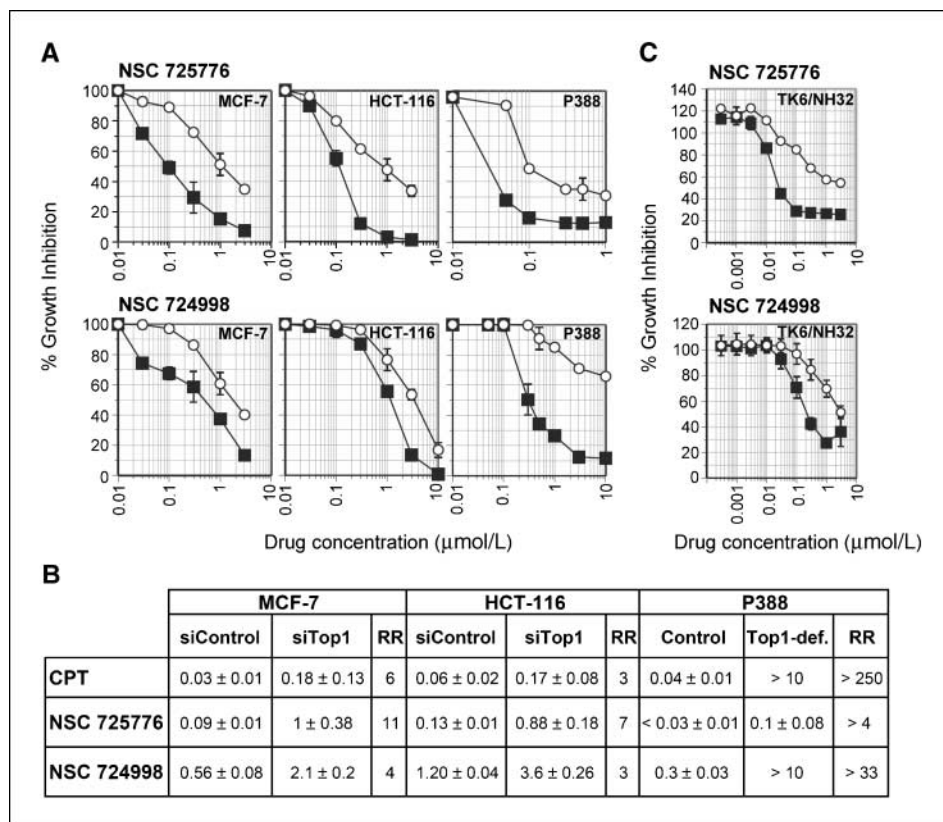
**Cytotoxicity of NSC 725776 and NSC 724998 is p53 dependent.** Consistent with previously published results (37), CPT-induced cell killing is p53 dependent (see ref. 26 for details). Loss of cell viability measured by cytotoxicity assay at 24 h of exposure to CPT showed an  $IC_{50}$  of  $\sim 5$  nmol/L for cells with wild-type p53 (TK6), whereas an  $IC_{50}$  of  $\sim 300$  nmol/L was observed for p53-null NH32 cells (data published in ref. 26). Similar to CPT, dependence on p53 was observed for both NSC 725776 and NSC 724998 (see Fig. 3C). NSC 725776 showed a 120-fold difference between the p53 wild-type and p53-null cells ( $IC_{50}$  of 25 nmol/L for TK6 and  $>3$   $\mu$ mol/L for NH32). NSC 724998 showed a 12-fold difference between the p53 wild-type and p53-null cells ( $IC_{50}$  of 250 nmol/L for TK6 and 1  $\mu$ mol/L for NH32). Overall, NSC 724998 showed the least toxicity and p53 dependence.

**NSC 725776 and NSC 724998 lead to cell cycle arrest in S and G<sub>2</sub>-M.** As known Top1 inhibitors, such as CPT or the indenoisoquinoline MJ-III-65 (NSC 706744), induce S-phase cell cycle arrest (4, 13, 38), we evaluated the effect of NSC 725776 and NSC 724998 on cell cycle progression. Human colon carcinoma HT29 cells were treated with varying doses of NSC 725776 and NSC 724998 for 6 h. At the lowest concentration used (0.01  $\mu$ mol/L), drug-treated cells accumulated in the G<sub>2</sub>-phase of the cell cycle (Fig. 4B and C). With increasing drug concentrations ( $\geq 0.05$   $\mu$ mol/L), the cells also showed an S-phase accumulation (Fig. 4B and C). This dose-dependent accumulation of cells in the S and G<sub>2</sub> phases of the cell cycle clearly indicates that both NSC 725776 and NSC 724998 exhibit cellular effects similar to known Top1 inhibitors.

**NSC 725776 but not NSC 724998 is a substrate for the transporter proteins ABCG2 and MDR-1.** Previous studies have shown that the ATP-binding cassette (ABC) transporter protein ABCG2 mediates resistance to the clinical CPT derivatives topotecan and SN-38 (active metabolite of irinotecan; refs. 8, 17). Additionally, topotecan is a P-glycoprotein (MDR-1) substrate as well (39). We sought to characterize and compare the effect of the ABC transporter family members ABCG2 and MDR-1 on NSC 725776-mediated and NSC 724998-mediated cytotoxicity relative to that of the CPT derivatives. Table 1 shows that cells overexpressing MDR-1 did not exhibit appreciable CPT resistance, whereas cell lines overexpressing the ABC half-transporter ABCG2 were found to be resistant to CPT, although not to a great extent (2-fold). However, the ABCG2-overexpressing cells were significantly resistant to the clinical CPT derivatives topotecan and SN-38 by approximately 9-fold and 46-fold, respectively. The indenoisoquinolines NSC 706744 and NSC 725776 were substrates of both ABCG2 (4- to 5-fold) and MDR-1 (2-fold). Strikingly, NSC 724998 was not a substrate to either ABCG2 or MDR-1. From these studies, we conclude that although the ABC transporters ABCG2 and MDR-1 confer cellular resistance to CPT derivatives, their role in NSC 725776-mediated and NSC 724998-mediated cytotoxicity is partial.

**Production of  $\gamma$ -H2AX foci in cells treated with NSC 725776 and NSC 724998.** Because phosphorylation of H2AX ( $\gamma$ -H2AX) is one of the early chromatin modifications induced by CPT and indicates formation of DNA double-stranded breaks (20, 21), we looked for  $\gamma$ -H2AX foci formation in HT29 cells treated with NSC 725776 and NSC 724998. Figure 5A shows  $\gamma$ -H2AX foci in cells treated for 1 h with NSC 725776 and NSC 724998 with drug concentrations as low as 100 nmol/L. The  $\gamma$ -H2AX staining increased as a function of dose. Additional experiments with cell cycle analysis

**Figure 3.** Partial resistance of Top1-siRNA, Top1-deficient, and p53-deficient cells to NSC 725776 and NSC 724998. **A**, growth inhibition in MCF-7 wild-type (■) and Top1-siRNA (○), HCT 116 wild-type (■) and Top1-siRNA (○), and P388 wild-type (■) and Top1-deficient (○) cells was measured by SRB or MTT assay after treatment with the indicated concentrations ( $\mu$ mol/L) of NSC 725776 or NSC 724998 for 3 d. **B**, the  $IC_{50}$  (concentration of drug that is required for 50% growth inhibition) of NSC 725776 and NSC 724998 in the three cell pairs in (A) is tabulated in micromolar concentrations. Effect of CPT is represented for comparison. **RR**, relative resistance value obtained by dividing the  $IC_{50}$  values of the Top1-siRNA or Top1-deficient cell line by the  $IC_{50}$  value of the respective parental cell line. Percentage of growth of several replicates from two independent experiments was averaged and represented as the mean  $\pm$  SD. **C**, percentage of growth of wild-type p53 (TK6; ■) and p53-null (NH32; ○) cells treated with indicated concentrations ( $\mu$ mol/L) of NSC 725776 and NSC 724998. Cells were plated in sextuplicate in 96-well tissue culture plates and treated with drugs for 24 h. Growth inhibition was measured as described in Materials and Methods. One of two independent experiments is shown.



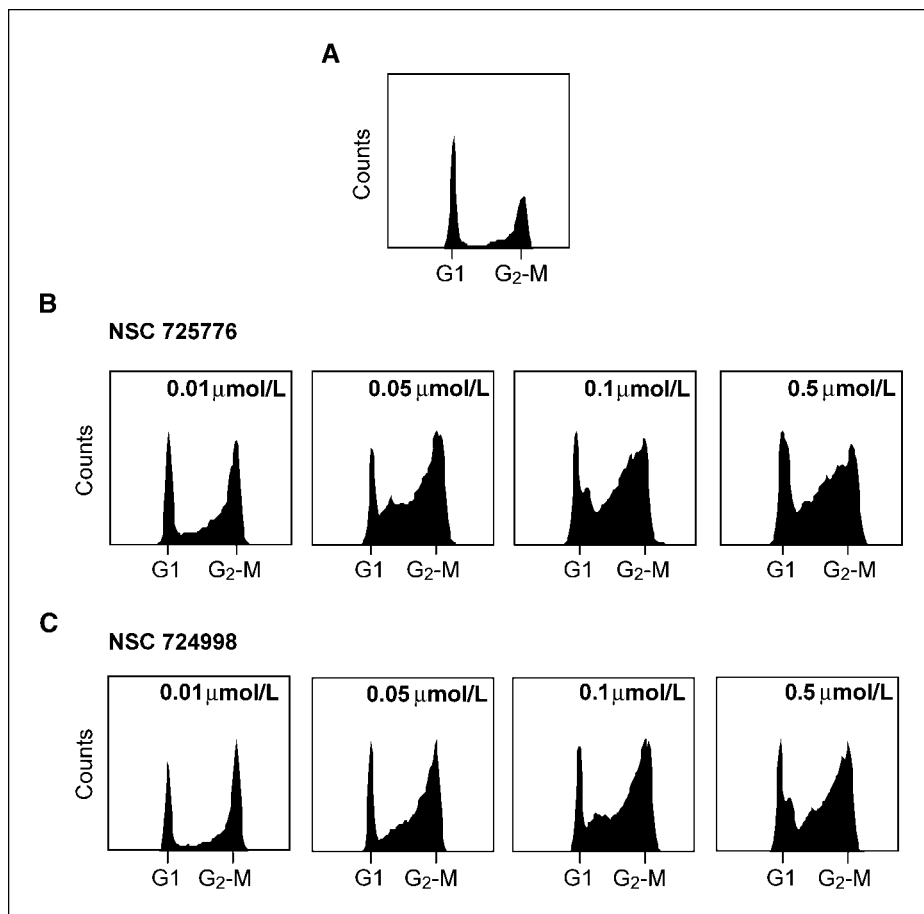


**Figure 4.** NSC 725776 and NSC 724998 arrest cells in both S and G<sub>2</sub>-M. HT29 cells were treated in the absence (A) or presence of indicated concentrations (μmol/L) of NSC 725776 (B) or NSC 724998 (C) for 6 h. Fixed cells were stained with propidium iodide and analyzed for DNA content distribution histograms by flow cytometry.

and quantification of  $\gamma$ -H2AX staining reveal that, like CPT, NSC 725776 and NSC 724998 treatment-induced  $\gamma$ -H2AX staining is predominantly in S-phase cells (Fig. 5B; ref. 21). To investigate the reversibility of  $\gamma$ -H2AX generated by NSC 725776 and NSC 724998, HT29 cells were first treated with NSC 725776, NSC 724998, and CPT (1 μmol/L for 1 h). After drug removal, cells were further incubated in drug-free medium for up to 24 h. As shown in Fig. 5C and Supplementary Fig. S2,  $\gamma$ -H2AX foci persisted for at least 24 h following drug treatment.  $\gamma$ -H2AX staining even increased approximately 4- to 7-fold after NSC 725776 and NSC 724998 removal. That increase was associated with the occurrence of cells with uniform nuclear  $\gamma$ -H2AX staining ("pan-staining"; Supplementary Fig. S2).

## Discussion

Because of the anticancer activity of CPTs (40, 41), many derivatives that inhibit Top1 have been synthesized for clinical development. Two of these have been approved by the FDA: topotecan (Hycamtin) for ovarian and lung cancers (42) and irinotecan (CPT11; Campto) for colon carcinomas (43). Several other derivatives are in preclinical development or clinical trial (exatecan, 9-nitrocamptothecin, and BAY 38-3441; ref. 4). Despite the success of CPT derivatives against solid tumors, their clinical limitations warrant the search for non-CPT Top1 inhibitors. The first indenoisoquinoline Top1 inhibitor, NSC 314622 (see Fig. 1A for structure), was identified after an analysis of its cytotoxicity profile revealed similarities to that of other known Top1 inhibitors (9). This correlation was confirmed by follow-up *in vitro* testing but indicated distinct differences of NSC 314622 to CPT (9). Notable

distinctions included chemical stability of the indenoisoquinolines, DNA cleavage site specificity, and Top1 cleavage complex stability (9). But the development of NSC 314622 as an anticancer agent was limited by its moderate potency both as a cytotoxic agent in cancer

**Table 1.** Relative resistance to CPTs, NSC 725776, and NSC 724998 in cell lines overexpressing ABCG2 and MDR-1 transporter proteins

Drug	IC <sub>50</sub> (nmol/L)	RR1	RR2	Drug efflux
CPT	19.6 ± 8.3	2-fold	1-fold	ABCG2
Topotecan	35.8 ± 7.5	9-fold	1-fold	ABCG2
SN-38	5.3 ± 1.2	46-fold	1-fold	ABCG2
NSC 706744	27.8 ± 13.3	4-fold	2-fold	ABCG2, P-gp
NSC 725776	8.5 ± 6.4	5-fold	2-fold	ABCG2, P-gp
NSC 724998	83.3 ± 46	1-fold	1-fold	None

NOTE: IC<sub>50</sub> values are in nanomolar concentrations. It represents the concentration of drug that is required for 50% growth inhibition of the parent cell line (HEK-293). Values obtained were from two separate experiments.

Abbreviations: RR1, relative resistance values obtained by dividing the IC<sub>50</sub> values of the ABCG2-overexpressing cell line (HEK-293-482R-5) by the IC<sub>50</sub> value of the respective parental cell line; RR2, relative resistance values obtained by dividing the IC<sub>50</sub> values of the MDR-1/P-glycoprotein-overexpressing cell line (HEK-293-MDR-19) by the IC<sub>50</sub> value of the respective parental cell line; P-gp, P-glycoprotein.

cells and as a Top1 inhibitor. Thus, several additional indenoisoquinolines related to NSC 314622 have been synthesized and evaluated for their cytotoxicity and Top1 inhibition (10–13, 26, 44–48). Of the indenoisoquinolines screened, among the most potent Top1 inhibitors were NSC 725776, NSC 724998, and the previously published NSC 706744 (13, 18). Those three indenoisoquinolines are currently in the pipeline for clinical trial at the NCI (23).

The present study was carried out to further characterize and determine the molecular mechanism by which NSC 725776 and NSC 724998 exert their activity in cellular systems. Structurally, NSC 725776 and NSC 724998 differ from the lead compound NSC 314622, NSC 706744, and each other by the substitution at the N6 position (see Fig. 1A). Based on the crystal structure, there exists a structural overlap between CPT and the indenoisoquinolines in their interaction with Top1-DNA complexes (14–16). Structural similarity could account for the trapping of DNA-Top1 cleavage

complexes at similar sites between CPT and the indenoisoquinolines NSC 725776, NSC 724998, and NSC 706744 (sites 70, 92, 97, and 119; Fig. 1B). However, both CPT and the indenoisoquinolines exhibit their uniqueness by preferential Top1-DNA trapping at unique sites (i.e., in Fig. 1B, sites 37 and 44). The potency of NSC 725776 and NSC 724998 increases with dose and is comparable with that of CPT, although differing in the sequence/cleavage sites preferred, which can be attributed to the side chain attached to the nitrogen N6 that protrudes in the DNA major groove (15).

Poisoning of the Top1-DNA cleavage complex by CPT does not occur at all Top1 cleavage sites along the DNA chain. The site selectivity exhibited by CPT is dependent on the bases immediately preceding (–1) and following (+1) the cleavage site. CPTs have a strict preference for a T (thymine) at the (–1) position and a preference for G (guanine or adenine) at the (+1) position of the Top1-mediated DNA cleavage site (Fig. 1B; ref. 49). NSC 725776 and

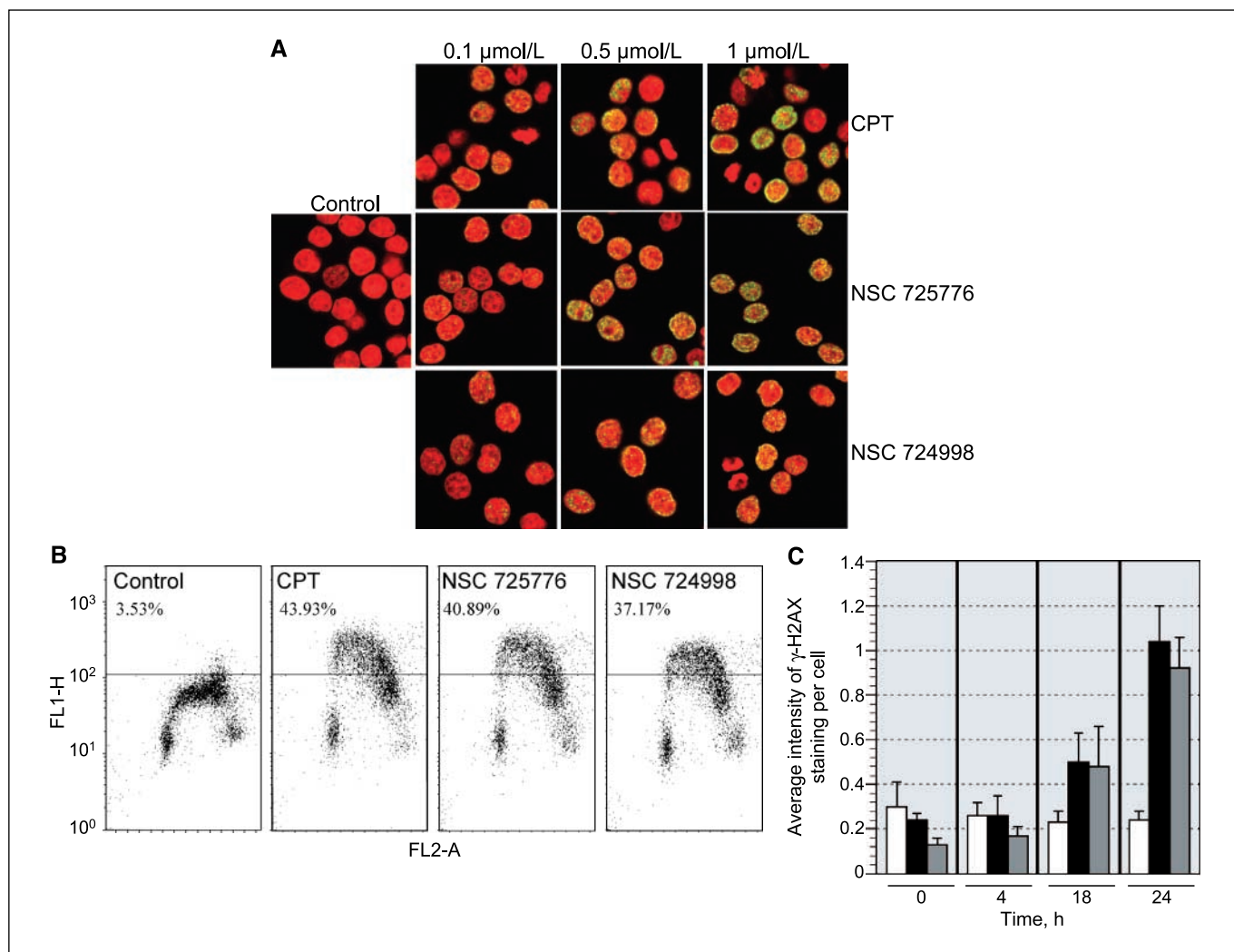


**Figure 5.** Generation of  $\gamma\text{-H2AX}$  foci in HT29 cells treated with NSC 725776 and NSC 724998. **A**, dose-dependent  $\gamma\text{-H2AX}$  formation. Cells were treated with the indicated concentrations of NSC 725776 or NSC 724998 or CPT for 1 h. *Green*, cells were stained with mouse anti- $\gamma\text{-H2AX}$  antibody and goat anti-mouse antibody conjugated with Alexa Fluor 488; *red*, nuclei were stained with propidium iodide. **B**, quantitation of  $\gamma\text{-H2AX}$  staining and cell cycle analysis were carried out by flow cytometry. Cells treated for 1 h with 1  $\mu\text{mol/L}$  of NSC 725776 or NSC 724998 or CPT were fixed and incubated with anti- $\gamma\text{-H2AX}$  antibody and propidium iodide. Scatter plots depict  $\gamma\text{-H2AX}$  labeling (Y axis, log scale) as a function of cell cycle distribution (X axis, propidium iodide content). *Numbers*, percentage of  $\gamma\text{-H2AX}$ -positive cells. **C**, irreversibility of  $\gamma\text{-H2AX}$  foci induced by NSC 725776 and NSC 724998. After treatment with 1  $\mu\text{mol/L}$  of NSC 725776 or NSC 724998 or CPT for 1 h, cells were further incubated in drug-free medium for the indicated times. Cells were stained with mouse anti- $\gamma\text{-H2AX}$  antibody and goat anti-mouse antibody conjugated with Alexa Fluor 488. Nuclei were stained with propidium iodide. *Columns*, mean average intensity of  $\gamma\text{-H2AX}$  staining per cell of several fields (each containing at least 50 cells) from two independent experiments; *bars*, SD.

NSC 724998 exhibit a relaxed preference at the  $-1$  (thymine or cytosine) and  $+1$  (adenine or guanine) positions (Fig. 1B; ref. 18). Such differences between indenoisoquinolines and CPTs may be important in cells because some genes may be more selectively targeted by one compound than the other, which may be translated into selective effects against various tumors. The concurrent use of both indenoisoquinolines and CPTs should also reveal a more complete picture of the Top1 cleavage/binding sites within the genome, which otherwise would have been restricted by using only one of the compounds.

We find that NSC 725776 and NSC 724998 also inhibit Top1 in human cells because Top1-DNA complexes were detected by the ICE bioassay (Fig. 2A) and by alkaline elution as DPCs (Fig. 2B). Therefore, NSC 725776 and NSC 724998 trap Top1 both in cell-free systems as well as in cells. Although CPT derivatives are also potent Top1 inhibitors in cells, they are limited by the rapid reversibility of the cleavage complexes on drug removal (5, 7), imposing prolonged drug administration. This is evidenced by the rapid reversibility of the Top1 cleavage complexes induced by CPT and its clinical derivatives topotecan and SN-38 (the active metabolite of irinotecan) following drug removal in cancer cells (see Fig. 2B and ref. 36). On the other hand, NSC 725776-induced and NSC 724998-induced Top1 cleavage complexes in cells persisted after drug removal, indicating stability of the NSC 725776-induced and NSC 724998-induced Top1-DNA complexes (Fig. 2B). Similarly, we previously reported that the Top1 cleavage complexes trapped by NSC 706744 reverse less rapidly than those induced by CPT (13, 18).

Like other known Top1 inhibitors such as CPT or the indenoisoquinoline NSC 706744, NSC 725776 and NSC 724998 depend on Top1 for exerting their cytotoxicity (Fig. 3A and B). CPT exhibits about a 3- and 6-fold resistance in the stable siRNA-mediated knockdown of Top1 in HCT-116 and MCF-7 cells (Fig. 3B; ref. 32). A similar fold decrease in the cytotoxicity of both NSC 725776 and NSC 724998 was observed in the Top1-siRNA cells (Fig. 3B). However, greater resistance of CPT, NSC 725776, and NSC 724998 was observed in the Top1-deficient P388 cells (Fig. 3B). The greater resistance in the Top1-deficient P388 cells compared with the HCT-116 and MCF-7 Top1-siRNA cells could be attributed to the fact that the P388 cells were generated by selectively growing them in the presence of increasing concentrations of CPT. They also show almost undetectable levels of Top1 protein (31). Moreover, as the P388 cells were selected in the presence of CPT, it is possible that those cells have additional resistance mechanism to CPT besides Top1 suppression. Based on these cellular studies, we infer that, like CPT, NSC 725776-mediated and NSC 724998-mediated cytotoxicity is primarily Top1 dependent.

Inhibition of Top1 leads to replication fork collision and DNA strand breaks (4). It is therefore not surprising that, like CPT (38) or NSC 706744 (38), NSC 725776 and NSC 724998 exhibit a dependence on wild-type p53 for cytotoxicity. The p53 tumor suppressor is an essential mediator of the cellular response to DNA damage. Its activation following DNA strand breaks, including those provoked by CPT-induced cleavage complexes, has been extensively characterized (38) and results in cell cycle arrest and apoptosis. Of the cell lines tested in this study, MCF-7 and HCT-116 bear wild-type *TP53*, whereas P388 carries an inactivating mutation. All of them exhibit Top1-dependent toxicity of NSC 725776 and NSC 724998. Thus, although the presence of wild-type p53 may increase their effect, even tumors carrying p53 mutations, a common source of chemotherapeutic resistance, are likely to

respond to NSC 725776 and NSC 724998. Consistent with Top1 inhibition, exposure to NSC 725776 or NSC 724998 led to early G<sub>2</sub>-M block followed by S-phase arrest (Fig. 4), similar to CPT (38). Altogether, these results indicate that Top1 is the primary target of NSC 725776 and NSC 724998 in cells. Nevertheless, it is not excluded that the indenoisoquinolines may affect additional targets, such as Top2 (Supplementary Fig. S1) and/or DNA (13).

Developing resistance to a drug during treatment is common and constitutes a major obstacle to the cure of potentially sensitive tumors. Although several resistance mechanisms are possible, one of the most common is increased efflux of the drug from the cell by ABC transporters. Consistent with previous studies (8, 17, 39), cells that overexpress ABCG2 and MDR-1 were significantly resistant to topotecan and SN-38 (Table 1). Whereas the indenoisoquinolines NSC 706744 and NSC 725776 are substrates of ABCG2 and MDR-1, NSC 724998 is not. Clearly, several differences exist within these indenoisoquinolines. All three indenoisoquinolines, NSC 725776, NSC 724998, and the previously published NSC 706744, depend on Top1 and p53 for their cytotoxicity. NSC 725776 and NSC 706744 are more potent and form relatively stable Top1-DNA cleavage complexes in cells but are substrates of the ABC transporters, whereas NSC 724998 is not a substrate for ABC transporters. The fact that the expression of ABC transporters only minimally affects NSC 724998-mediated cytotoxicity confers an advantage for clinical development. Thus, individual differences among the indenoisoquinolines could be exploited in treating tumors by combination therapy.

Although Top1 and p53 status are crucial determinants of NSC 725776 and NSC 724998 toxicity, their levels cannot be used as a marker to determine the efficacy of these drugs in tumors. H2AX phosphorylation (at its COOH terminus on Ser<sup>139</sup>;  $\gamma$ -H2AX) appears within minutes after ionizing radiation (50), and  $\gamma$ -H2AX focus formation is considered to be a sensitive and selective signal for formation of DNA double-strand breaks. As previously published, within an hour of CPT treatment,  $\gamma$ -H2AX is formed in cells as a response to replication-induced double-strand break (20, 21). We could also detect  $\gamma$ -H2AX foci on NSC 725776 and NSC 724998 treatment at a concentration as low as 0.1  $\mu$ mol/L (Fig. 5). Additionally, the  $\gamma$ -H2AX foci induced on NSC 725776 and NSC 724998 treatment persisted for at least 24 h and even increased in intensity, indicating a persistent DNA damage (Fig. 5C; "pan-staining pattern" in Supplementary Fig. S2). Thus, it should be possible to measure  $\gamma$ -H2AX in tumor samples several hours following 1-h drug infusions.  $\gamma$ -H2AX may be a useful clinical marker for monitoring the efficacy of NSC 725776 and NSC 724998 in tumor therapies. Studies are ongoing to validate  $\gamma$ -H2AX in animal models (Proceedings of the American Association for Cancer Research, vol. 48, page 953, April 2007). Clinical trials will be needed to determine whether  $\gamma$ -H2AX is a useful pharmacodynamic biomarker to monitor the activity of the indenoisoquinolines NSC 725776 and NSC 724998 in cancer patients.

## Acknowledgments

Received 3/15/2007; revised 8/16/2007; accepted 9/6/2007.

**Grant support:** NIH Research Grant U01 CA89566, Training Grant ST32 CA09634-12, ACS Medicinal Chemistry Predoctoral Fellowship sponsored by Pfizer Global Research and Development (A. Morrell), and contract NO1-CO-56000 through the Developmental Therapeutics Program, Division of Cancer Treatment and Diagnosis, NCI. This research was also supported in part by the Intramural Research Program of the NIH, NCI, Center for Cancer Research.

The costs of publication of this article were defrayed in part by the payment of page charges. This article must therefore be hereby marked *advertisement* in accordance with 18 U.S.C. Section 1734 solely to indicate this fact.

## References

- Hsiang YH, Hertzberg R, Hecht S, Liu LF. Camptothecin induces protein-linked DNA breaks via mammalian DNA topoisomerase I. *J Biol Chem* 1985;260:14873-8.
- Nitiss J, Wang JC. DNA topoisomerase-targeting antitumor drugs can be studied in yeast. *Proc Natl Acad Sci U S A* 1988;85:7501-5.
- Froelich-Ammon SJ, Osheroff N. Topoisomerase poisons: harnessing the dark side of enzyme mechanism. *J Biol Chem* 1995;270:21429-32.
- Pommier Y. Topoisomerase I inhibitors: camptothecins and beyond. *Nat Rev Cancer* 2006;6:789-802.
- Covey JM, Jaxel C, Kohn KW, Pommier Y. Protein-linked DNA strand breaks induced in mammalian cells by camptothecin, an inhibitor of topoisomerase I. *Cancer Res* 1989;49:5016-22.
- Burke TG, Mi Z. The structural basis of camptothecin interactions with human serum albumin: impact on drug stability. *J Med Chem* 1994;37:40-6.
- Staker BL, Hjerrild K, Feese MD, Behnke CA, Burgin AB, Jr., Stewart L. The mechanism of topoisomerase I poisoning by a camptothecin analog. *Proc Natl Acad Sci U S A* 2002;99:15387-92.
- Brangi M, Litman T, Ciotti M, et al. Camptothecin resistance: role of the ATP-binding cassette (ABC), mitoxantrone-resistance half-transporter (MXR), and potential for glucuronidation in MXR-expressing cells. *Cancer Res* 1999;59:5938-46.
- Kohlhagen G, Paull KD, Cushman M, Nagafuji P, Pommier Y. Protein-linked DNA strand breaks induced by NSC 314622, a novel noncamptothecin topoisomerase I poison. *Mol Pharmacol* 1998;54:50-8.
- Cushman M, Jayaraman M, Vroman JA, et al. Synthesis of new indeno[1,2-*c*]isoquinolines: cytotoxic non-camptothecin topoisomerase I inhibitors. *J Med Chem* 2000;43:3688-98.
- Fox BM, Xiao X, Antony S, et al. Design, synthesis, and biological evaluation of cytotoxic 11-alkenylindenoisoquinoline topoisomerase I inhibitors and indenoisoquinoline-camptothecin hybrids. *J Med Chem* 2003;46:3275-82.
- Strumberg D, Pommier Y, Paull K, Jayaraman M, Nagafuji P, Cushman M. Synthesis of cytotoxic indenoisoquinoline topoisomerase I poisons. *J Med Chem* 1999;42:446-57.
- Antony S, Kohlhagen G, Agama K, et al. Cellular topoisomerase I inhibition and antiproliferative activity by MJ-III-65 (NSC 706744), an indenoisoquinoline topoisomerase I poison. *Mol Pharmacol* 2005;67:523-30.
- Ioanoviciu A, Antony S, Pommier Y, Staker BL, Stewart L, Cushman M. Synthesis and mechanism of action studies of a series of norindenoisoquinoline topoisomerase I poisons reveal an inhibitor with a flipped orientation in the ternary DNA-enzyme-inhibitor complex as determined by X-ray crystallographic analysis. *J Med Chem* 2005;48:4803-14.
- Marchand C, Antony S, Kohn KW, et al. A novel norindenoisoquinoline structure reveals a common interfacial inhibitor paradigm for ternary trapping of the topoisomerase I-DNA covalent complex. *Mol Cancer Ther* 2006;5:287-95.
- Staker BL, Feese MD, Cushman M, et al. Structures of three classes of anticancer agents bound to the human topoisomerase I-DNA covalent complex. *J Med Chem* 2005;48:2336-45.
- Rajendra R, Gounder MK, Saleem A, et al. Differential effects of the breast cancer resistance protein on the cellular accumulation and cytotoxicity of 9-amino-camptothecin and 9-nitrocamptothecin. *Cancer Res* 2003;63:3228-33.
- Antony S, Jayaraman M, Laco G, et al. Differential induction of topoisomerase I-DNA cleavage complexes by the indenoisoquinoline MJ-III-65 (NSC 706744) and camptothecin: base sequence analysis and activity against camptothecin-resistant topoisomerases I. *Cancer Res* 2003;63:7428-35.
- Tanizawa A, Kohn KW, Kohlhagen G, Leteurtre F, Pommier Y. Differential stabilization of eukaryotic DNA topoisomerase I cleavable complexes by camptothecin derivatives. *Biochemistry* 1995;34:7200-6.
- Huang X, Traganos F, Darzynkiewicz Z. DNA damage induced by DNA topoisomerase I- and topoisomerase II-inhibitors detected by histone H2AX phosphorylation in relation to the cell cycle phase and apoptosis. *Cell Cycle* 2003;2:614-9.
- Furuta T, Takemura H, Liao ZY, et al. Phosphorylation of histone H2AX and activation of Mre11, Rad50, and Nbs1 in response to replication-dependent DNA double-strand breaks induced by mammalian DNA topoisomerase I cleavage complexes. *J Biol Chem* 2003;278:20303-12.
- Gorgoulis VG, Vassiliou LV, Karakaidos P, et al. Activation of the DNA damage checkpoint and genomic instability in human precancerous lesions. *Nature* 2005;434:907-13.
- Kummar S, Kinders R, Rubinstein L, et al. Compressing drug development timelines in oncology using phase 0 trials. *Nat Rev Cancer* 2007;7:131-9.
- Cushman M, Cheng L. A stereoselective oxidation by thionyl chloride leading to the indeno[1,2-*c*] isoquinoline system. *J Org Chem* 1978;43:3781.
- Nagarajan M, Morrell A, Ioanoviciu A, et al. Synthesis and evaluation of indenoisoquinoline topoisomerase I inhibitors substituted with nitrogen heterocycles. *J Med Chem* 2006;49:6283-9.
- Antony S, Agama KK, Miao ZH, et al. Bisindenoisoquinoline bis-1,3-((5,6-dihydro-5,11-diketo-11H-indeno[1,2-*c*]isoquinoline)-6-propylamino)propane bis(trifluoroacetate) (NSC 727357), a DNA intercalator and topoisomerase inhibitor with antitumor activity. *Mol Pharmacol* 2006;70:1109-20.
- Kohn KW. DNA filter elution: a window on DNA damage in mammalian cells. *Bioessays* 1996;18:505-13.
- Shaw JL, Blanco J, Mueller GC. Simple procedure for isolation of DNA, RNA and protein fractions from cultured animal cells. *Anal Biochem* 1975;65:125-31.
- Subramanian D, Kraut E, Staubs A, Young DC, Muller MT. Analysis of topoisomerase I/DNA complexes in patients administered topotecan. *Cancer Res* 1995;55:2097-103.
- Sordet O, Khan QA, Plo I, et al. Apoptotic topoisomerase I-DNA complexes induced by staurosporine-mediated oxygen radicals. *J Biol Chem* 2004;279:50499-504.
- Mattern MR, Hofmann GA, McCabe FL, Johnson RK. Synergistic cell killing by ionizing radiation and topoisomerase I inhibitor topotecan (SK&F 104864). *Cancer Res* 1991;51:5813-6.
- Miao ZH, Player A, Shankavaram U, et al. Non-classical functions of human topoisomerase I: genome-wide and pharmacological analyses. *Cancer Res* 2007;67:8752-61.
- Robey RW, Honjo Y, Morisaki K, et al. Mutations at amino-acid 482 in the ABCG2 gene affect substrate and antagonist specificity. *Br J Cancer* 2003;89:1971-8.
- Pourquier P, Takebayashi Y, Urasaki Y, Gioffre C, Kohlhagen G, Pommier Y. Induction of topoisomerase I cleavage complexes by 1- $\beta$ -D-arabinofuranosylcytosine (ara-C) *in vitro* and in ara-C-treated cells. *Proc Natl Acad Sci U S A* 2000;97:1885-90.
- Kohn KW, Shao RG, Pommier Y. How do drug-induced topoisomerase I-DNA lesions signal to the molecular interaction network that regulates cell cycle checkpoints, DNA replication, and DNA repair? *Cell Biochem Biophys* 2000;33:175-80.
- Tanizawa A, Fujimori A, Fujimori Y, Pommier Y. Comparison of topoisomerase I inhibition, DNA damage, and cytotoxicity of camptothecin derivatives presently in clinical trials. *J Natl Cancer Inst* 1994;86:836-42.
- Li G, Bush JA, Ho VC. p53-dependent apoptosis in melanoma cells after treatment with camptothecin. *J Invest Dermatol* 2000;114:514-9.
- Shao RG, Cao CX, Shimizu T, O'Connor PM, Kohn KW, Pommier Y. Abrogation of an S-phase checkpoint and potentiation of camptothecin cytotoxicity by 7-hydroxystaurosporine (UCN-01) in human cancer cell lines, possibly influenced by p53 function. *Cancer Res* 1997;57:4029-35.
- Hoki Y, Fujimori A, Pommier Y. Differential cytotoxicity of clinically important camptothecin derivatives in P-glycoprotein-overexpressing cell lines. *Cancer Chemother Pharmacol* 1997;40:433-8.
- Garcia-Carbonero R, Supko JG. Current perspectives on the clinical experience, pharmacology, and continued development of the camptothecins. *Clin Cancer Res* 2002;8:641-61.
- Wall ME, Wani MC. Camptothecin and taxol: discovery to clinic—thirteenth Bruce F. Cain Memorial Award Lecture. *Cancer Res* 1995;55:753-60.
- Garst J. Safety of topotecan in the treatment of recurrent small-cell lung cancer and ovarian cancer. *Expert Opin Drug Saf* 2007;6:53-62.
- Fuchs C, Mitchell EP, Hoff PM. Irinotecan in the treatment of colorectal cancer. *Cancer Treat Rev* 2006;32:491-503.
- Jayaraman M, Fox BM, Hollingshead M, Kohlhagen G, Pommier Y, Cushman M. Synthesis of new dihydroindeno[1,2-*c*]isoquinoline and indenoisoquinolinium chloride topoisomerase I inhibitors having high *in vivo* anticancer activity in the hollow fiber animal model. *J Med Chem* 2002;45:242-9.
- Morrell A, Antony S, Kohlhagen G, Pommier Y, Cushman M. Synthesis of nitrated indenoisoquinolines as topoisomerase I inhibitors. *Bioorg Med Chem Lett* 2004;14:3659-63.
- Nagarajan M, Morrell A, Fort BC, et al. Synthesis and anticancer activity of simplified indenoisoquinoline topoisomerase I inhibitors lacking substituents on the aromatic rings. *J Med Chem* 2004;47:5651-61.
- Nagarajan M, Xiao X, Antony S, Kohlhagen G, Pommier Y, Cushman M. Design, synthesis, and biological evaluation of indenoisoquinoline topoisomerase I inhibitors featuring polyamine side chains on the lactam nitrogen. *J Med Chem* 2003;46:5712-24.
- Xiao X, Antony S, Kohlhagen G, Pommier Y, Cushman M. Design, synthesis, and biological evaluation of cytotoxic 11-aminoalkenylindenoisoquinoline and 11-diaminoalkenylindenoisoquinoline topoisomerase I inhibitors. *Bioorg Med Chem* 2004;12:5147-60.
- Jaxel C, Capranico G, Kerrigan D, Kohn KW, Pommier Y. Effect of local DNA sequence on topoisomerase I cleavage in the presence or absence of camptothecin. *J Biol Chem* 1991;266:20418-23.
- Rogakou EP, Pilch DR, Orr AH, Ivanova VS, Bonner WM. DNA double-stranded breaks induce histone H2AX phosphorylation on serine 139. *J Biol Chem* 1998;273:5858-68.

### **Correction: Topoisomerase I Inhibition by NSC 725776 and NSC 724998**

In the article on topoisomerase I inhibition by NSC 725776 and NSC 724998 in the November 1, 2007 issue of *Cancer Research* (1), the legend of Fig. 5C is missing the color code for the columns. It should be as follows: *white*, camptothecin; *black*, NSC 725776; *grey*, NSC 724998.

1. Antony S, Agama KK, Miao Z-H, Takagi K, Wright MH, Robles AI, Varticovski L, Nagarajan M, Morrell A, Cushman M, Pommier Y. Novel idenoisoquinolines NSC 725776 and NSC 724998 produce persistent topoisomerase I cleavage complexes and overcome multidrug resistance. *Cancer Res* 2007;67:10397-405.

# Cancer Research

The Journal of Cancer Research (1916–1930) | The American Journal of Cancer (1931–1940)

## Novel Indenoisoquinolines NSC 725776 and NSC 724998 Produce Persistent Topoisomerase I Cleavage Complexes and Overcome Multidrug Resistance

Smitha Antony, Keli K. Agama, Ze-Hong Miao, et al.

*Cancer Res* 2007;67:10397-10405.

<b>Updated version</b>	Access the most recent version of this article at: <a href="http://cancerres.aacrjournals.org/content/67/21/10397">http://cancerres.aacrjournals.org/content/67/21/10397</a>
<b>Supplementary Material</b>	Access the most recent supplemental material at: <a href="http://cancerres.aacrjournals.org/content/suppl/2007/12/11/67.21.10397.DC1">http://cancerres.aacrjournals.org/content/suppl/2007/12/11/67.21.10397.DC1</a>

<b>Cited articles</b>	This article cites 50 articles, 23 of which you can access for free at: <a href="http://cancerres.aacrjournals.org/content/67/21/10397.full#ref-list-1">http://cancerres.aacrjournals.org/content/67/21/10397.full#ref-list-1</a>
<b>Citing articles</b>	This article has been cited by 23 HighWire-hosted articles. Access the articles at: <a href="http://cancerres.aacrjournals.org/content/67/21/10397.full#related-urls">http://cancerres.aacrjournals.org/content/67/21/10397.full#related-urls</a>

<b>E-mail alerts</b>	<a href="#">Sign up to receive free email-alerts</a> related to this article or journal.
<b>Reprints and Subscriptions</b>	To order reprints of this article or to subscribe to the journal, contact the AACR Publications Department at <a href="mailto:pubs@aacr.org">pubs@aacr.org</a> .
<b>Permissions</b>	To request permission to re-use all or part of this article, use this link <a href="http://cancerres.aacrjournals.org/content/67/21/10397">http://cancerres.aacrjournals.org/content/67/21/10397</a> . Click on "Request Permissions" which will take you to the Copyright Clearance Center's (CCC) Rightslink site.